Molecular Therapy
Nucleic Acids
Original Article

# SIRT1 alleviates hepatic ischemia-reperfusion injury via the miR-182-mediated XBP1/NLRP3 pathway

Fengwei Li,[1,3] Lei Zhang,[1,3] Hui Xue,[1] Jianbing Xuan,[1] Shu Rong,[2] and Kui Wang[1]

[1]Department of Hepatic Surgery (II), Eastern Hepatobiliary Surgery Hospital, Naval Medical University (Second Military Medical University), Shanghai 200438, P.R. China; [2]Department of Nephrology, Shanghai General Hospital, Shanghai Jiao Tong University School of Medicine, Shanghai 200080, P.R. China

**The hepatoprotection of histone deacetylase sirtuin 1 (SIRT1) has been identified to attenuate ischemia-reperfusion (IR)-triggered inflammation and liver damage. This study was performed to characterize the function of SIRT1 in hepatic IR injury. In *in vivo* assays on liver-specific knockout mice of SIRT1, we first validated the effect of SIRT1 knockout on liver damage and XBP1/NLRP3 inflammasome activation. Next, we examined whether knockdown of XBP1/NLRP3 or miR-182 agomir could reverse the effect of SIRT1 knockout. In *in vitro* assays, NCTC1469 cells subjected to hypoxia/reoxygenation (H/R) were transduced with small interfering RNA (siRNA)/activator of SIRT1 or miR-182 agomir to confirm the effect of SIRT1 on NCTC1469 cell behaviors as well as the regulation of miR-182 and the XBP1/NLRP3 signaling pathway. Hepatic IR injury was appreciably aggravated in SIRT1 knockout mice, and SIRT1 knockdown abolished the inhibition of XBP1/NLRP3 inflammasome activation, which was reversed by NLRP3 knockdown, XBP1 knockdown, or miR-182 agomir. Mechanistically, miR-182 expression was positively regulated by SIRT1 in hepatic IR injury in mice, and miR-182 inhibited the expression of XBP1 by binding to the 3′ untranslated region (UTR) of XBP1. The histone deacetylase SIRT1 inhibits the downstream XBP1/NLRP3 inflammatory pathway by activating miR-182, thus alleviating hepatic IR injury in mice.**

## INTRODUCTION

Hepatic ischemia-reperfusion (IR) injury induces high morbidity and mortality of patients following liver resection and transplantations[1,2] As reported, it is the leading cause of liver dysfunction and failure after liver surgery or transplantation, and satisfactory strategies to ameliorate hepatic IR injury are limited.[3] Emerging studies have unraveled the involvement of significant cell death and inflammatory responses[4] and oxidative stress and tissue damage[5] in hepatic IR injury. Interestingly, NLRP3 inflammasome activation has been reported to possess a critical function in hepatic IR injury.[6,7] Notably, researchers have demonstrated that inflammatory signaling inhibition can improve liver function and lower hepatocyte apoptosis and neutrophil infiltration.[8,9] Still, the molecular causes leading to such inhibition are poorly understood, and effective treatments have been slow to emerge.

Recently, there has been exceptional interest in the interaction of microRNAs (miRNAs) and inflammatory signaling pathways, especially where attention has also focused on their potential for use as biomarkers to support early diagnosis and prognosis in the clinic.[10,11] Of note, miRNA-182-5p (miR-182-5p) has been proposed to suppress liver damage and inflammation by targeting Toll-like receptor 4 (TLR4) in an animal model of hepatic IR injury and a cell model of lipopolysaccharide-induced inflammation.[12] In addition, the anti-inflammatory effect of miR-182-5p has been proven in cerebral IR injury by repressing release of tumor necrosis factor-α (TNF-α), interleukin (IL)-6, and IL-1β.[13] Intriguingly, Wang et al.[14] pointed out that miR-182 is a downstream effector of sirtuin 1 (SIRT1), and SIRT1 binds to the miR-182 promoter and regulates its transcription. SIRT1 is a histone deacetylase whose activation often functions as a mediator affecting the inflammatory reaction and suppressing liver damage following hepatic IR injury.[15] Moreover, activation of SIRT1 represses cellular inflammation by restricting NLRP3 inflammasome formation and IL-1β production.[16] The evidence presented by Inoue et al.[17] documented that hepatic IR could elevate the production of the inflammasome component NLRP3, which in turn leads to accelerated reactive oxygen species production and hepatocyte apoptosis in IR liver. Additionally, hepatic XBP1 expression is implicated in the adaptive response to endoplasmic reticulum stress in the liver, leading to the control of liver injury, hepatocyte apoptosis, and liver fibrosis.[18] This study aims to delineate new mechanisms by which a histone deacetylase, SIRT1, exerts its beneficial effects against

Received 10 July 2020; accepted 20 November 2020;
https://doi.org/10.1016/j.omtn.2020.11.015.

[3]These authors contributed equally

**Correspondence:** Kui Wang, Department of Hepatic Surgery (II), Eastern Hepatobiliary Surgery Hospital, Naval Medical University (Second Military Medical University), No. 225, Changhai Road, Yangpu District, Shanghai 200438, P.R. China.
**E-mail:** wangkuiykl@163.com
**Correspondence:** Shu Rong, Department of Nephrology, Shanghai General Hospital, Shanghai Jiao Tong University School of Medicine, No. 100, Haining Road, Hongkou District, Shanghai 200080, P.R. China.
**E-mail:** sophiars@126.com

 © 2020 The Authors.
This is an open access article under the CC BY-NC-ND license (http://creativecommons.org/licenses/by-nc-nd/4.0/).

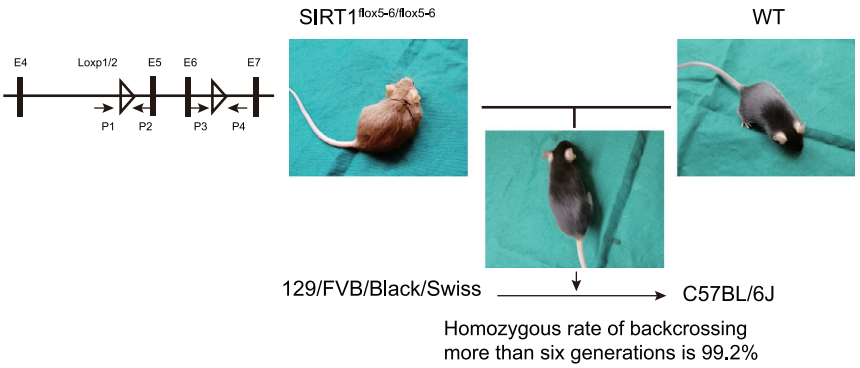


**Figure 1. Backcrossing changes the genetic background of SIRT1$^{flox5-6/flox5-6}$ mice**

hepatic IR injury in mouse models of hepatic IR. miR-182 and the XBP1/NLRP3 inflammatory pathway appear to be potential targets of SIRT1.

## RESULTS

### SIRT1 knockout aggravated hepatic IR injury in mice

In an attempt to investigate whether SIRT1 regulates the downstream miR-182/XBP1/NLRP3 pathway in hepatic IR injury, we established a SIRT1 overexpression or knockout mouse model (Figures 1 and 2). Although the experimental method of establishing SIRT1 knockout mice has been largely reported, it is still very difficult to screen the overexpression animal model. Therefore, we decided to use SIRT1 knockout mice as our main experimental animals in the study. We established hepatocyte-specific SIRT1 knockout mice via hybridization of SIRT1$^{flox5-6/flox5-6}$ with Alb-Cre mice. First, the SIRT1 knockout efficiency was verified. After extraction of the DNA from the tail tissues of mice, PCR amplification was performed, followed by agarose gel electrophoresis (AGE). Subsequently, an ultraviolet imager was applied to capture the images, and the results regarding the loxP locus of SIRT1 were identified as follows: (1) homozygote: there were loxP loci on a pair of homologous chromosomes; the AGE image showed only one large band; (2) heterozygote: only one homologous chromosome had a loxP locus on the ultraviolet image; there were two bands on the AGE image; and (3) wild-type (WT): there was no loxP locus on both homologous chromosomes on the ultraviolet image, and there was only one band on the AGE image. The identification of the Cre gene (Figure 3A) showed that only mice with amplifiable-specific bands were Cre mice, and only SIRT1$^{flox5-6/flox5-6}$ homozygous mice expressing Cre recombinase could be SIRT1-LKO mice (liver-specific knockout mice of SIRT1), while those without Cre recombinase expression were used as WT control mice. Quantitative reverse-transcriptase PCR (qRT-PCR) and western blot analysis results showed that the SIRT1 expression decreased significantly in the liver of SIRT1 knockout mice ($p < 0.01$) (Figures 3B and 3C). After that, we established the hepatic IR model in SIRT1 knockout mice and WT control mice at the same time and evaluated the IR injury by detecting the serum liver function and through H&E staining, TUNEL (terminal deoxynucleotidyltransferase [TdT]-mediated deoxyuridine triphosphate nick end labeling) staining, and immunohistochemistry. In the IR mouse model, compared with that in WT control mice, the serum level of alanine aminotransferase (ALT) in SIRT1 knockout mice displayed a notable increase (Figure 3D). In addition, H&E staining for livers showed that congestion, vacuolation, and necrosis all increased significantly in the liver of SIRT1 knockout mice in comparison to those in the liver of WT control mice (Figure 3E). As illustrated in TUNEL staining and immunohistochemistry, SIRT1 knockout mice also showed significantly increased hepatocyte apoptosis ($p < 0.05$) (Figure 3F) as well as an elevated immunohistochemical optical density (IOD) value relative to the WT control mice (Figure 3G).

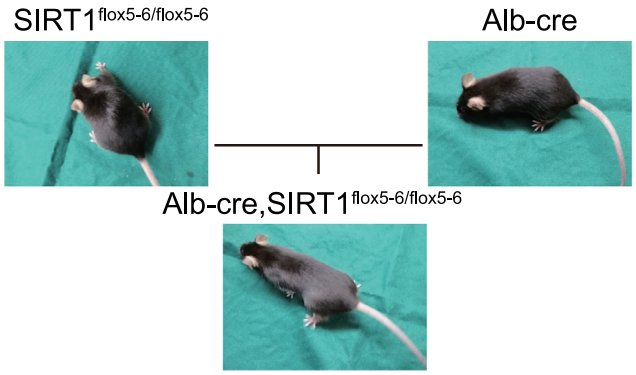


**Figure 2. Hybrid SIRT1 knockout mice are obtained from hybridizing**

### SIRT1 knockout activated the XBP1/NLRP3 inflammatory pathway

Subsequently, we explored whether the role of the XBP1/NLRP3 inflammatory pathway in hepatic IR injury is regulated by SIRT1. qRT-PCR and western blot analysis were conducted to detect the expression of the key proteins of the XBP1/NLRP3 inflammatory pathway, namely, XBP1, NLRP3, cleaved caspase-1, caspase-activating recruitment domain (ASC), and nuclear factor κB (NF-κB), and enzyme-linked immunosorbent assay (ELISA) was used to determine the expression of the relevant inflammatory factors (IL-1β, TNF-α, and IL-18) in the liver of mice in response to different treatment. From the results, mice subjected to IR showed a marked elevation with regard to the expression of key proteins and relevant inflammatory factors of the XBP1/NLRP3 inflammatory pathway relative to the sham-operated mice. Moreover, SIRT1 knockout further upregulated expression of key proteins and related inflammatory factors in the XBP1/NLRP3 inflammatory pathway in mice subjected to IR (Figures 4A–4C). Therefore, it was demonstrated that SIRT1 knockout could aggravate hepatic IR injury in mice by activating the XBP1/NLRP3 inflammatory pathway.

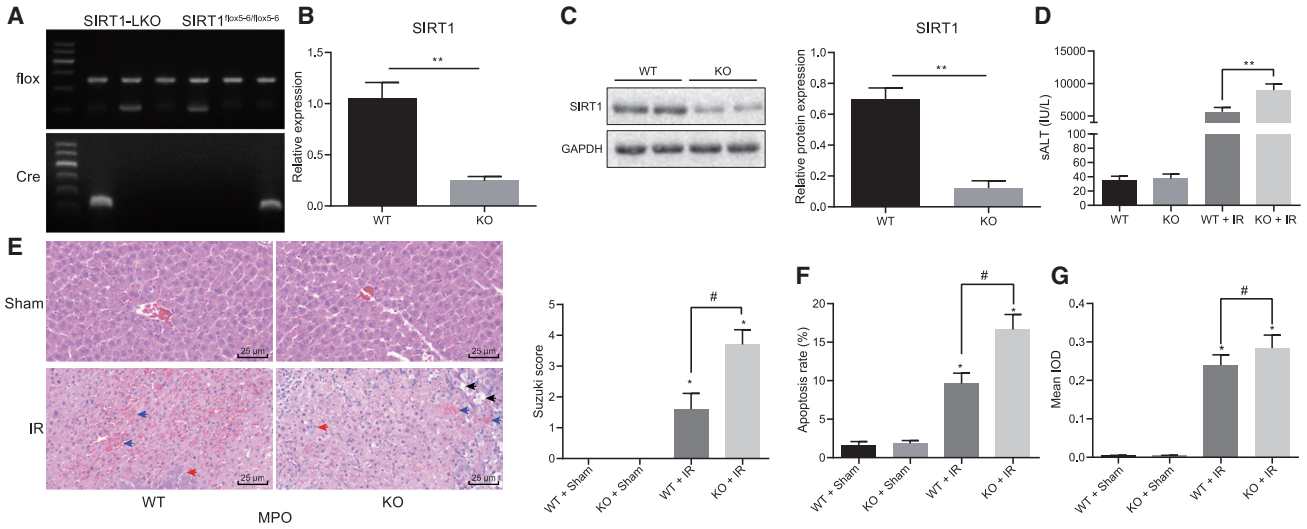


**Figure 3. SIRT1 knockout aggravates hepatic IR injury in mice**

(A) Genotypes of SIRT1 and Cre. (B) Expression of SIRT1 in liver of WT control mice and SIRT1 knockout mice as detected by qRT-PCR. (C) Protein expression of SIRT1 in liver of WT control mice and SIRT1 knockout mice as detected by western blot analysis, normalized to GAPDH. (D) Serum ALT level of WT control mice and SIRT1 knockout mice as detected using a specific detection kit. (E) Histomorphology of the liver in WT control mice and SIRT1 knockout mice as observed by H&E staining (original magnification, ×400) and scoring of the IR injury based on Suzuki et al.'s[19] standard. (F) Apoptosis of hepatocytes in WT control mice and SIRT1 knockout mice as observed by TUNEL staining and the calculated apoptotic rate. (G) The Expression of MPO as detected by immunohistochemistry. *$p < 0.05$, **$p < 0.01$ versus the sham-operated WT mice or knockout mice; #$p < 0.05$, ##$p < 0.01$ versus WT control mice subjected to IR. The data are measurement data, presented as mean ± standard deviation. Data between two groups were compared using an unpaired t test. The experiment was independently repeated three times. n = 10. KO, knockout.

### Silencing of NLRP3 reversed the aggravating effect of SIRT1 knockout on hepatic IR injury in mice

In this part of the experiment, we used NLRP3 small interfering RNA (siRNA) in SIRT1 knockout mice to further confirm the regulatory effect of SIRT1 on the XBP1/NLRP3 inflammatory pathway. First, western blot analysis confirmed the good transfection efficiency of NLRP3 siRNA (Figure 5A). Next, the results from H&E staining, TUNEL staining, and immunohistochemistry demonstrated that the use of NLRP3 siRNA contributed to a markedly reduced degree of liver injury, ameliorated histomorphology, reduced hepatocyte apoptosis, and decreased myeloperoxidase (MPO) expression (Figures 5B–5D). Additionally, silencing of NLRP3 markedly reduced serum ALT level and IL-1β concentration (Figures 5E and 5F). These results further confirmed that silencing of NLRP3 was able to reverse the aggravating effect of SIRT1 knockout on hepatic IR injury in mice.

### Silencing of XBP1 reversed the aggravating effect of SIRT1 knockout on mice hepatic IR injury via inhibition of the NLRP3 inflammatory pathway

Furthermore, XBP1 siRNA was used in SIRT1 knockout mice to further verify the regulatory effect of SIRT1 on the XBP1/NLRP3 inflammatory pathway. Western blot results confirmed the good silencing efficiency of XBP1 siRNA (Figure 6A). In addition, it was evident that the use of XBP1 siRNA led to a notable decline in the degree of liver injury, an amelioration in terms of histomorphology, as well as decreases in the serum ALT level (Figures 6B and 6C). Moreover, we used ELISA and western blot analysis to detect the expression of the NLRP3 inflammatory pathway-related proteins and inflammatory factors. From the results, SIRT1 knockout mice treated with XBP1 siRNA displayed marked decreases with regard to the expression of NLRP3 inflammatory pathway-related proteins (NLRP3, ASC, C-caspase-1, and NF-kB) and inflammatory factors (IL-1β, TNF-α, and IL-18) (Figures 6D and 6E). Therefore, it was confirmed that the silencing of XBP1 was capable of reversing the aggravating effect of SIRT1 knockout on hepatic IR injury in mice via inhibition of the NLRP3 inflammatory pathway.

### miR-182 expression was positively regulated by SIRT1 in mice with hepatic IR injury

Whether SIRT1 also plays a protective role by regulating miR-182 in the hepatic IR injury model was then explored. We first detected the miRNA expression profile of WT control mice and SIRT1 knockout mice using the miRNA microarray profile. It was found that after SIRT1-specific knockout, the expression of miR-182 was significantly reduced (Figure 7A). We then continued to determine the expression of SIRT1 and miR-182 in the WT control mice subjected to sham operation or IR. Based on the results, the expression of SIRT1 and miR-182 in the WT control mice subjected to IR was notably lower than that in the WT control mice subjected to sham operation (Figure 7B). Since the experimental animals we used were hepatocyte-specific SIRT1 knockout mice, in order to simulate the hepatic IR injury *in vitro*, we used the normal mouse NCTC1469 hepatocytes to establish the hypoxia/reoxygenation (H/R) model, aiming to further verify

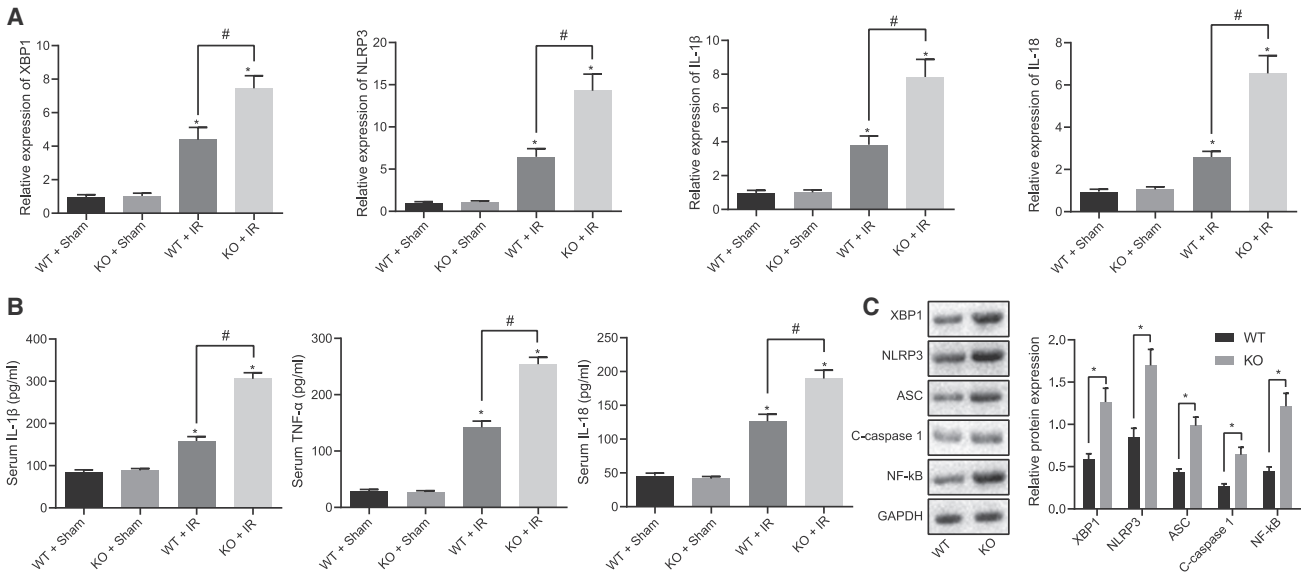


**Figure 4. SIRT1 knockout activates the XBP1/NLRP3 inflammatory pathway**

(A) mRNA expression of XBP1, NLRP3, IL-1β, and IL-18 in liver of WT control mice and SIRT1 knockout mice both in response to different treatment. (B) The levels of IL-1β, TNF-α, and IL-18 in the serum of WT control mice and SIRT1 knockout mice both in response to different treatment as detected by ELISA. (C) The protein expression of XBP1, NLRP3, C-caspase-1, ASC, and NF-κB in liver of WT control mice and SIRT1 knockout mice both in response to different treatment as detected by western blot analysis as well as the corresponding histogram. *$p < 0.05$, **$p < 0.01$ versus the sham-operated WT mice or knockout mice; #$p < 0.05$, ##$p < 0.01$ versus WT control mice subjected to IR. The data are measurement data, presented as mean ± standard deviation. Data between two groups were compared using an unpaired t test. The experiment was independently repeated three times. n = 10.

the relationship between IR and SIRT1 and miR-182. The results revealed that the expression of SIRT1 and miR-182 in NCTC1469 hepatocytes in mice undergoing H/R was significantly lower than that in hepatocytes in sham-operated mice (Figure 7C). Two different SIRT1 activators, SRT1720 and resveratrol (RSV), were used to treat the cultured NCTC1469 hepatocytes, and the expression of SIRT1 and miR-182 was detected. As revealed by the results, SRT1720 and RSV could upregulate SIRT1 and miR-182 expression (Figure 7D). After NCTC1469 hepatocytes were activated with SRT1720 and RSV, we established an H/R model and detected the expression of SIRT1 and miR-182. After qRT-PCR, we found that SRT1720 and RSV could upregulate SIRT1 and miR-182 on the basis of the established H/R model relative to non-treatment or DMSO treatment (Figure 7E). Next, we silenced or overexpressed SIRT1 using adenovirus and detected the expression of miR-182 again. The results demonstrated that miR-182 was notably upregulated after SIRT1 overexpression but downregulated after SIRT1 silencing (Figure 7F). Through the dual-luciferase reporter gene assay, we found that the relative luciferase activity of miR-182 was elevated with the increase of SIRT1 transfected into the cells, showing that SIRT1 could promote the gene expression of miR-182 by combining with the promoter of miR-182 (Figure 7G). Finally, a chromatin immunoprecipitation assay was performed to evaluate the binding activity of SIRT1 to the miR-182 promoter from chromatin of mouse hepatocytes. The results in Figure 7H demonstrated that SIRT1 was integrated into the predicted promoter region. Collectively, these results suggested that the expression of miR-182 could be positively regulated by SIRT1 in mice with hepatic IR injury.

### miR-182 downregulated the expression of XBP1 in mice with hepatic IR

Furthermore, we continued to verify whether XBP1 mouse hepatic IR injury is regulated by miR-182, in order to further confirm the integrity of the SIRT1/miR-182/XBP1/NLRP3 pathway. Through a dual-luciferase reporter gene assay, we found that miR-182 could notably inhibit the expression of XBP1 by binding with its untranslated region (UTR) region (Figure 8A). Next, we further verified the inhibitory effect of miR-182 on the protein expression of XBP1 with the use of *in vitro*-cultured hepatocytes (Figure 8B). Finally, the inhibitory effect of miR-182 on the protein expression of XBP1 in hepatic IR injury was verified by establishing a mouse hepatocyte H/R model (Figure 8C).

### Overexpression of miR-182 counteracted the aggravating effect of SIRT1 knockout on hepatic IR injury in mice by inhibiting the NLRP3 inflammatory pathway

In this part of the experiment, we used miR-182 agomir in SIRT1 knockout mice to further confirm that SIRT1 regulates the XBP1/NLRP3 inflammatory pathway through miR-182. We first found that compared with SIRT1 knockout mice treated with agomir negative treated control (NTC), SIRT1 knockout mice treated with miR-182 agomir had a significantly reduced degree of liver injury,

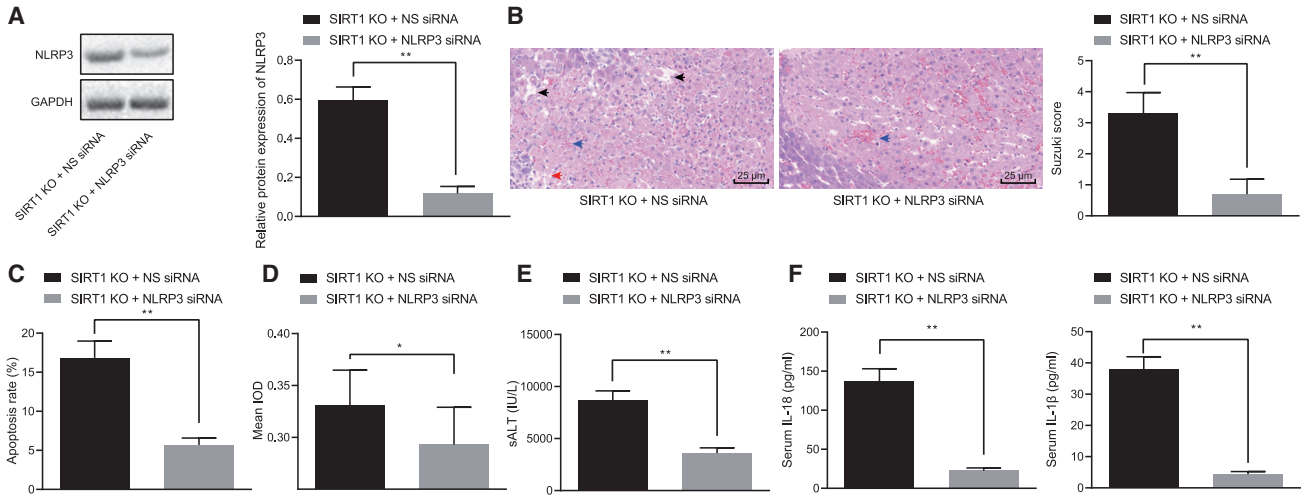


**Figure 5. Depletion of NLRP3 reverses the aggravating effect of SIRT1 knockout on hepatic IR injury in mice**

(A) Silencing efficiency of NLRP3 siRNA detected by western blot analysis as well as the corresponding histogram. (B) Liver histomorphology of SIRT1 knockout mice treated with NS siRNA or NLRP3 siRNA, and scoring of the hepatic IR injury based on Suzuki et al.'s[19] standard (original magnification, ×400). (C) Apoptosis of hepatocytes detected by TUNEL staining. (D) MPO expression detected by immunohistochemistry and statistics of mean IOD. (E) Serum ALT level of SIRT1 knockout mice treated with NS siRNA or NLRP3 siRNA as detected using a specific detection kit. (F) Levels of IL-1β and IL-18 in serum of SIRT1 knockout mice treated with NS siRNA or NLRP3 siRNA as measured by ELISA. *$p < 0.05$ versus SIRT1 knockout mice treated with NS siRNA; **$p < 0.01$ versus SIRT1 knockout mice treated with NS siRNA. The data are measurement data, presented as mean ± standard deviation. Data between two groups were compared using an unpaired t test. The experiment was independently repeated three times. n = 10.

ameliorated histomorphology, and decreased the serum ALT level (Figures 9A and 9B). Additionally, qRT-PCR confirmed the transfection efficiency of miR-182 agomir (Figure 9C). Furthermore, the results from qRT-PCR and western blot analysis displayed that the expression of the XBP1/NLRP3 inflammatory pathway-related proteins (XBP1, NLRP3, ASC, C-caspase-1, and NF-κB) and inflammatory factors (IL-1β, TNF-α, and IL-18) was markedly lower in SIRT1 knockout mice treated with miR-182 agomir than in those treated with agomir NTC (Figures 9D and 9E).

## DISCUSSION

Hepatic IR injury leads to irreversible liver damage to individuals who have received liver resection or transplantation surgeries, especially in those with diseased livers.[20,21] Recent evidence provided by Nakamura et al.[15] from mouse models and human samples has validated the SIRT1-mediated hepatoprotection in curbing leukocyte infiltration and proinflammatory cytokine release in mice, as well as improved hepatocellular function and survival in human liver transplants. Thus, therapeutic improvements may come from fresh approaches associated with SIRT1, but knowledge of the mechanisms by which it acts is still very limited. This study clarified that SIRT1 confers hepatoprotective effects against hepatic IR injury by targeting the miR-182/XBP1/NLRP3 axis.

We first verified that SIRT1 knockout aggravated hepatic IR injury in mice. SIRT1 is a $NAD^+$-dependent protein deacetylase, and its induction is associated with multiple physiological processes, including cellular stress response and immune response.[22] SIRT1 deacetylates proteins implicated in the cellular stress response, including those related to IR injury.[23] In addition, SIRT1 activation was demonstrated by the study of Nakamura et al.[24] to rescue livers from IR-induced damage and hepatocellular death through restoring the p53 signaling.

Furthermore, our findings uncovered that the detrimental effects of SIRT1 knockout on liver functions were realized through activating the XBP1/NLRP3 inflammatory pathway. The NLRP3-mediated inflammasome represents a significant effector in innate immunity, and it results in facilitated production of proinflammatory cytokines in inflammation-related diseases.[16] Meanwhile, silencing of NLRP3 reversed the aggravating effect of SIRT1 knockout on hepatic IR injury in mice. A prior study has pointed to the importance of fully characterizing the NLRP3-dependent and inflammasome-independent pathway in the development of IR injury in the kidney.[25] Recent evidence indicates that siRNA-mediated SIRT1 knockdown appreciably diminished cell autophagy activity and restricted NLRP3 inflammasome activation in rat models of cerebral IR.[26] Another study on rat models of metabolic syndrome has suggested that SIRT1 overexpression and repression of NF-κB/NLRP3 inflammasome induction abrogate renal glomerular injury by diminishing inflammatory cell infiltration and IL-1β production.[27] A study on NLRP3-deficient mice validated the relieved hepatic IR injury upon NLRP3 ablation.[6] Furthermore, we found that silencing XBP1 reversed the aggravating effect of SIRT1 knockout on hepatic IR injury in mice via inhibition of the NLRP3 inflammatory pathway. In a mouse model of IR-triggered liver inflammation, facilitated NLRP3/caspase-1 activity and XBP1/NLRP3 activation were witnessed, while XBP1 ablation diminished

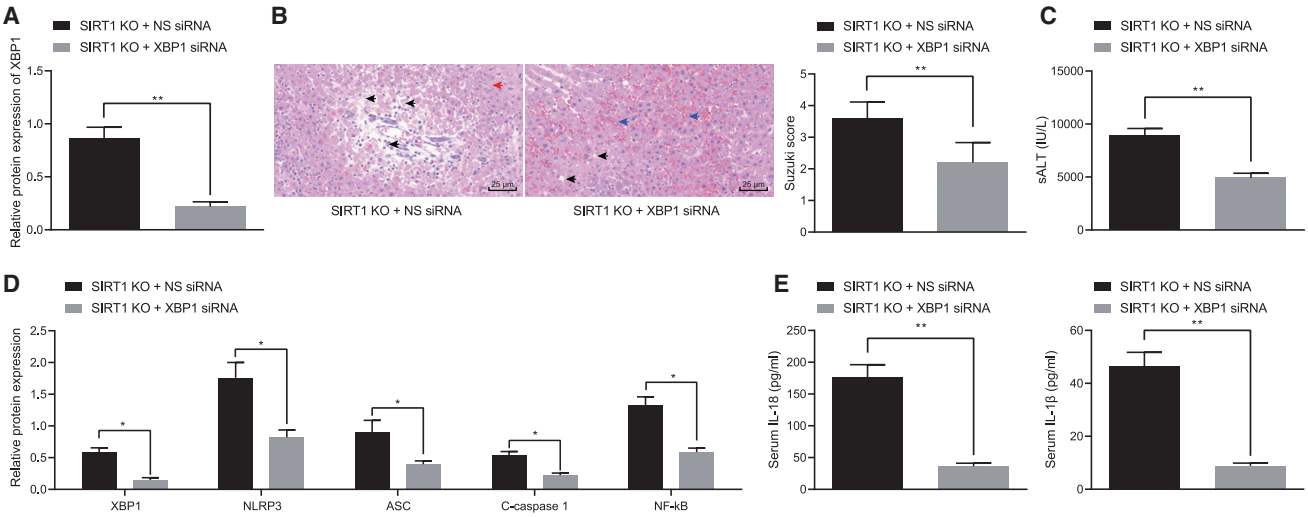


**Figure 6. Silencing of XBP1 reverses the aggravating effect of SIRT1 knockout on mice hepatic IR injury via inhibition of the NLRP3 inflammatory pathway**

(A) Silencing efficiency of XBP1 siRNA detected by western blot analysis. (B) Liver histomorphology of SIRT1 knockout mice treated with NS siRNA or XBP1 siRNA, and scoring of the hepatic IR injury based on Suzuki et al.'s[19] standard (original magnification, ×400). (C) Serum ALT level of SIRT1 knockout mice treated with NS siRNA or XBP1 siRNA as detected using a specific detection kit. (D) Protein expression of NLRP3 and C-caspase-1 in SIRT1 knockout mice treated with NS siRNA or XBP1 siRNA as detected by western blot analysis, normalized to GAPDH. (E) Levels of IL-1β and IL-18 in serum of SIRT1 knockout mice treated with NS siRNA or XBP1 siRNA as measured by ELISA. *$p < 0.05$ versus SIRT1 knockout mice treated with NS siRNA, **$p < 0.01$ versus SIRT1 knockout mice treated with NS siRNA. The data are measurement data, presented as mean ± standard deviation. Data between two groups were compared using an unpaired t test. The experiment was independently repeated three times. n = 10.

the NLRP3/caspase-1 activity, leading to reduced IL-1β release.[28] Additionally, STF-083010, as an inhibitor of XBP1 splicing, has been suggested to alleviate impairments caused by endoplasmic reticulum stress in IR-induced acute renal failure by restricting cell apoptosis and inflammation.[29]

Further mechanistic investigations showed that SIRT1 positively regulated the expression of miR-182, which was found to repress the expression of XBP1 in mice with hepatic IR injury. The presence of miR-182-5p overexpression resulted in diminished TNF-α and IL-6 production, thus attenuating hepatic IR injury by negatively regulating TLR4.[12] Lee et al.[30] has indicated that miR-182 suppressed IR-induced cardiac cell death by targeting and downregulating BNIP3. These findings were consistent with our results that miR-182 overexpression could impede the hepatic IR injury in mice. Prior evidence also highlighted that the expression level of miR-182 is positively regulated by SIRT1 due to its binding to the miR-182 promoter.[14] Therefore, it is rational to conclude that the alleviatory effect of SIRT1 on liver damage may implicate the regulation of miR-182. More importantly, we unraveled that overexpression of miR-182 counteracted the aggravating effect of SIRT1 knockout on hepatic IR injury in mice by inhibiting the NLRP3 inflammatory pathway. Previous studies have demonstrated the function of miRNAs in the control of the NLRP3 inflammatory pathway in the context of liver inflammation; for example, miR-200a-mediated TXNIP/NLRP3 inflammasome inactivation led to curbed hepatic inflammation in rat models.[31] Another miRNA, miR-223, blocked the activation of the NLRP3 inflammasome in a mouse model of endotoxin acute hepatitis, mitigating the acute and chronic liver injury.[32] In the present study, the NLRP3 inflammasome activation was suppressed by miR-182 overexpression, which resulted in alleviated liver damage.

In conclusion, our study gives new insight into the hepatoprotective mechanisms of SIRT1 in hepatic IR injury, implying that SIRT1 might be an important mediator of these beneficial effects. SIRT1 ablation promotes hepatic IR injury by impairing miR-182-mediated XBP1/NLRP3 pathway inactivation (Figure 10). By targeting innate and adaptive immune activation, manipulation of SIRT1 signaling should be considered as a novel means to combat inflammation triggered by IR in liver transplantation.

## MATERIALS AND METHODS

### Ethics statement

The study was conducted under the approval of the Ethics Committee of Eastern Hepatobiliary Surgery Hospital, Navy Medical University (Second Military Medical University). All animal experiments were conducted in accordance with the Animal Management Regulations published by the State Science and Technology Commission of the PRC in 2017 and the *Guide for the Care and Use of Laboratory Animals* published by the National Institutes of Health in 2011. Extensive efforts were made to ensure minimal suffering of the animals used during the study.

### Experimental animals

Five SIRT1$^{flox5\text{-}6/flox5\text{-}6}$ mice with a genetic background of 129/FVB/Black/Swiss were purchased from Shanghai SLAC Laboratory Animal

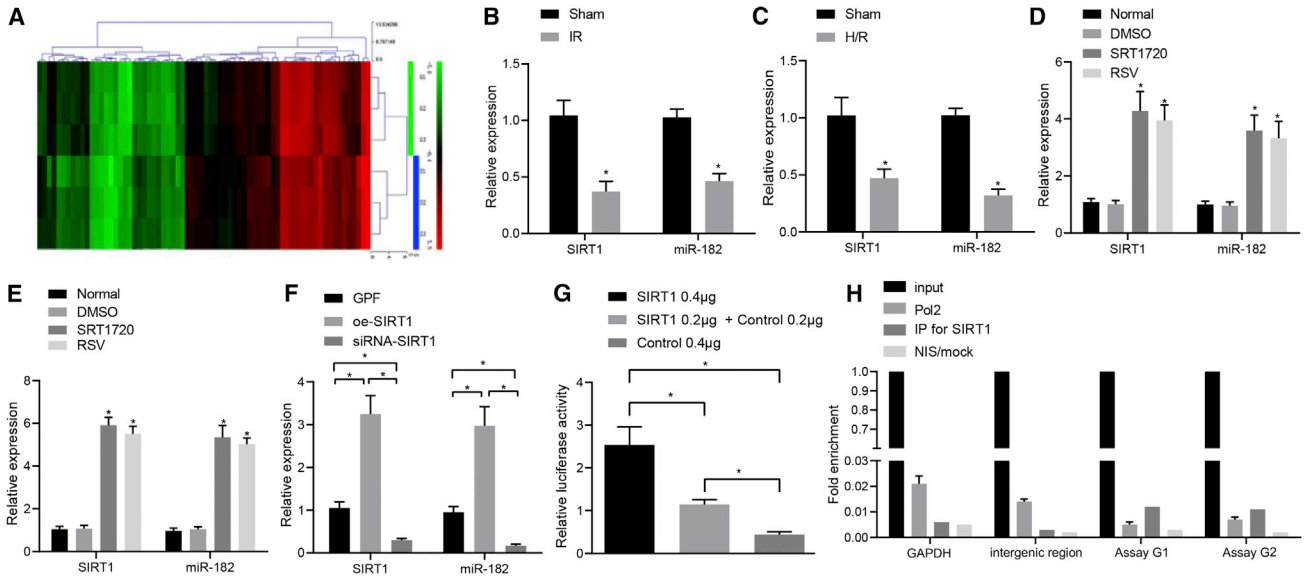


**Figure 7. miR-182 expression is positively regulated by SIRT1 in mice with hepatic IR injury**

(A) miRNA expression profile of WT control mice and SIRT1 knockout mice as detected through microarray profiling. Group G refers to WT control mice; group S refers to SIRT1 knockout mice. (B) miR-182 expression in WT control mice subjected to sham operation or IR as detected by qRT-PCR. (C) Expression of SIRT1 and miR-182 in NCTC1469 hepatocytes in mice undergoing H/R and sham-operated mice as detected by qRT-PCR, normalized to GAPDH. (D) miR-182 expression in NCTC1469 cells processed using SRT1720 and RSV detected by qRT-PCR. (E) NCTC1469 cells were induced by SRT1720 and RSV, followed by establishment of H/R model. Samples were collected after modeling, and qRT-PCR was used to detect the expression of miR-182. (F) Adenovirus was used to overexpress or interfere with SIRT1 in NCTC1469 cells, and qRT-PCR was used to detect the expression of miR-182. (G) Binding of SIRT1 and the miR-182 promoter as detected by a dual-luciferase reporter gene assay. (H) Binding activity of SIRT1 to miR-182 promoter from chromatin of mouse hepatocytes as detected by ChIP assay. *$p < 0.05$. These data are measurement data, expressed as mean ± standard deviation. Data between two groups were compared using an unpaired t test. Data among multiple groups were compared using one-way analysis of variance and then analyzed with Tukey's post hoc test. The experiment was repeated three times.

(Shanghai, China). Alb-Cre transgenic mice (with a genetic background of C57BL/6JJ) specifically expressing Cre recombinase in hepatocytes were purchased from Jackson Laboratory (Bar Harbor, ME, USA) (Figure 1). SIRT1$^{flox5\text{-}6/flox5\text{-}6}$ and C57BL/6J WT mice were hybridized and backcrossed for more than six generations, making their background become C57BL/6J. The SIRT1$^{flox5\text{-}6}$/Alb-Cre mice were hybridized with SIRT1$^{flox5\text{-}6/flox5\text{-}6}$ mice to obtain SIRT1$^{flox5\text{-}6/flox5\text{-}6}$ Alb-Cre mice and the control SIRT1$^{flox5\text{-}6/flox5\text{-}6}$ mice in the same nest[33–35] (Figure 2).

### Experimental grouping

SIRT1$^{flox5\text{-}6/flox5\text{-}6}$ homozygous mice expressing Cre recombinase were SIRT1-LKO mice, while those without Cre recombinase expression were used as WT control mice. All of the experimental animals were fed in a specific pathogen-free environment and fasted for 12 h before modeling. Based on the time of hepatic ischemia, the mice were sham operated or subjected to IR (60-min ischemia and then 24-h reperfusion).[2,36] First, it was verified whether SIRT1 knockout could affect hepatic IR injury and the XBP1/NLRP3 inflammatory pathway. The experimental mice were assigned into the following groups: sham-operated WT control mice, sham-operated SIRT1 knockout mice, WT control mice subjected to IR, and SIRT1 knockout mice subjected to IR (n = 10). Second, we verified whether NLRP3 or XBP1 siRNA could counteract the effect of SIRT1 knockout on hepatic IR injury in mice. Therefore, the SIRT1 knockout mice were treated with non-specific (NS) siRNA, NLRP3 siRNA, or XBP1 siRNA (n = 10). Next, we explored whether the expression of miR-182 was regulated by SIRT1 in mice with hepatic IR injury, with the experimental mice assigned into sham-operated WT control mice, sham-operated SIRT1 knockout mice, WT control mice subjected to IR, and SIRT1 knockout mice subjected to IR (n = 10).

For the cell experiment, hepatocytes were grouped as follows: (1) hepatocytes were used only as normal hepatocytes without any treatment, or treated with SIRT1 knockdown, subjected to H/R, or both treated with silencing of SIRT1 and subjected to H/R; (2) hepatocytes were used only as normal hepatocytes without any treatment, or treated with dimethyl sulfoxide (DMSO), SRT1720 (activator of SIRT1), or RSV (activator of SIRT1); (3) hepatocytes used for H/R modeling did not undergo treatment or were further treated with DMSO, SRT1720, or RSV; (4) hepatocytes were used only as normal hepatocytes without any treatment, or treated with overexpression or silencing of SIRT1; and (5) normal hepatocytes were treated with 0.4 μg of SIRT1 interference plasmid, 0.2 μg of SIRT1 interference plasmid, and 0.2 μg of control plasmid, or 0.4 μg of control plasmid.

Finally, in order to verify whether the XBP1/NLRP3 inflammatory pathway is regulated by miR-182 in mice with hepatic IR injury,

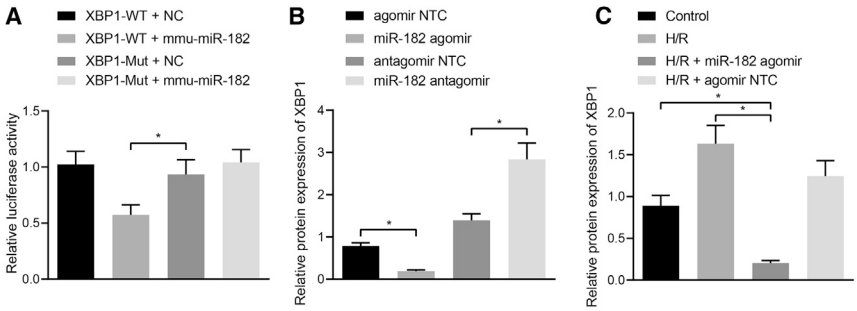


**Figure 8. miR-182 downregulates the expression of XBP1 in mice with hepatic IR**

(A) miR-182 binding site in 3′ UTR of XBP1 as evaluated by a dual-luciferase reporter gene assay. After 48 h of co-transfection, luciferase activity was detected by calculating fluorescence intensity. (B) Detection of the expression of XBP1 in mouse hepatocytes after transfection of miR-182 agomir or miR-182 antagomir by western blot analysis. (C) On the basis of transfection of the miR-182 agomir into cultured mouse hepatocytes, a hepatocyte H/R model was established, followed by detection of the expression of XBP1 in mouse hepatocytes by western blot analysis. *$p < 0.05$. These data are measurement data, expressed as mean ± standard deviation. Data among multiple groups were compared using one-way analysis of variance and then analyzed with Tukey's post hoc test. The experiment was repeated three times.

the SIRT1 knockout mice were treated with agomir NTC or miR-182 agomir (n = 10), XBP1-WT + miRNA, XBP1-WT + miR-182, XBP1-KO + control miRNA, or XBP1-KO + miR-182 (n = 10). Meanwhile, normal hepatocytes were further treated with control agomir, miR-182 agomir, antagomir, or miR-182 antagomir; the hepatocytes used for H/R model establishment were treated with miR-182 agomir or control agomir.

### Model establishment of 70% hepatic IR

Mice in the experimental group were anesthetized by intraperitoneal injection of pentobarbital sodium (50 mg/kg) and fixed on a heating plate. Povidone-iodine (PVI) (5%) was used for disinfection after skin removal and skin preparation of the abdominal wall. The abdominal viscera were exposed through a medial longitudinal incision. The section of the mouse liver was carefully identified with an operating microscope, and the specific positions of the left lobe and the middle lobe of the liver were determined. The small intestines and other organs near the porta hepatis were gently pushed to the left iliac region with a cotton swab (moistened with salt water), and then the porta hepatis was dissociated. A microvascular clamp was used to clamp the common trunk of the vein vessels in the left and middle lobes of the liver in order to make these lobes ischemic, thereby achieving 70% ischemia of the liver tissues. At this time, the color of the ischemic liver lobes changed, observable under the direct vision of the naked eyes. The remaining 30% of the liver lobes, namely the right lobe and the caudate lobe, were given smooth blood circulation, so as to prevent mesenteric vein congestion. After confirmation of the successful occlusion of blood flow, the abdominal cavity was temporarily closed, and the abdominal wall incision was covered with wet gauze to avoid fluid loss. Meanwhile, the temperature was monitored through rectal temperature probes, and the temperature was maintained at 37°C through a heating plate and a heating lamp. After the ischemic process reached the predetermined time, the microvascular clamp was removed to start the reperfusion, and a 4-0 polypropylene thread suture was used for continuous suturing. During the operation, the temperature of mice was monitored using an animal temperature maintenance instrument to maintain a constant temperature. Sham-operated mice did not undergo clamping of vessels. At the end of the observation period after reperfusion, these mice were anesthetized with inhaled methoxyflurane and euthanized by artery bloodletting.

In the *in vivo* siRNA interference experiment, 4 h before ischemia, the SIRT1 knockout mice were injected with Alexa Fluor 488-labeled siRNA or a mixture of NLRP3 siRNA (2 mg/kg) and mannose-conjugated polymer via the tail vein, followed by the model establishment of 70% hepatic IR.

### Model establishment of mouse hepatocytes with H/R

Normal mouse NCTC1469 hepatocytes were purchased from the Navy Medical University (Second Military Medical University). Cells were subcultured with Dulbecco's modified Eagle's medium (DMEM) containing high-glucose medium and 10% fetal bovine serum (FBS) in an incubator at 37°C with 5.0% $CO_2$. The day prior to H/R model establishment, the $O_2$ concentration of the three-gas incubator was set at 94%, the $CO_2$ concentration at 5%, and the $N_2$ concentration was set at 94%; the temperature was set at 37°C, with constant 40% humidity. Cells were taken out from the normal incubator on the day of experiment, and the culture medium was replaced with ischemic culture medium (98.5 mmol/L NaCl, 10.0 mmol/L KCl, 0.9 mmol/L $NaH_2PO_4$, 6.0 mmol/L $NaHCO_3$, 1.8 mmol/L $CaCl_2$, 1.2 mmol/L $MgSO_4$, 40.0 mmol/L sodium lactate, and 20.0 mmol/L HEPES with the pH value of 6.8). The incubator was then put into an anoxic culture device. The timing started upon each indicator became stable, and the cultured cells were taken out from the incubator after 24 h of hypoxia treatment. When the cells were treated with reoxygenation, the ischemic culture solution in the cell culture bottle was poured out and then supplemented with DMEM containing high glucose and 10% FBS. Finally, the cells were cultured in an incubator at 37°C with 5.0% $CO_2$ for 12 h.

### Construction of SIRT1 plasmids and transfection of mouse hepatocytes

Mouse SIRT1 overexpression plasmid, SIRT1 siRNA, and the corresponding control sequence were designed, synthesized, and sequenced by the Navy Medical University (Second Military Medical

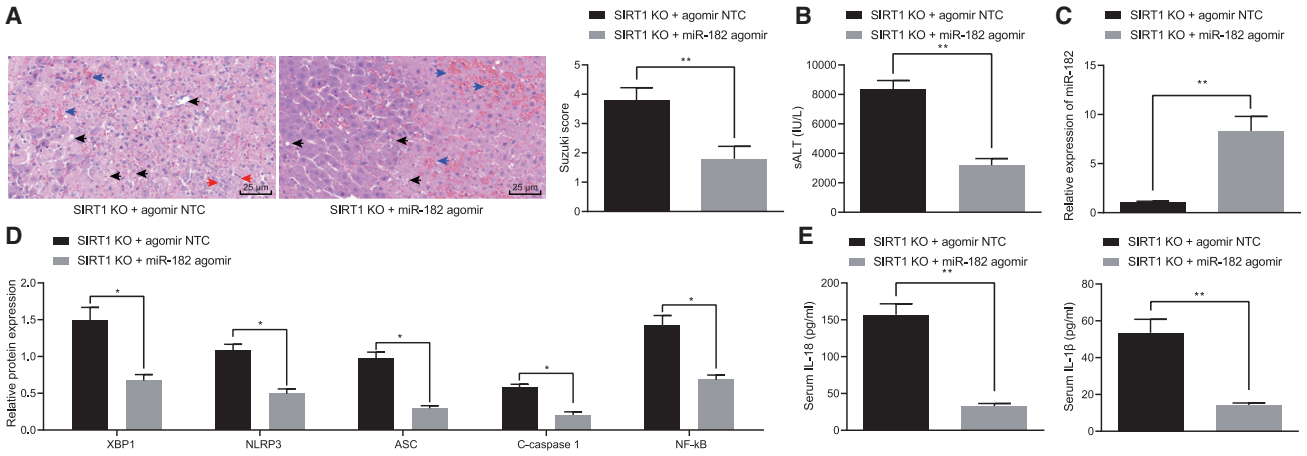


**Figure 9. Overexpression of miR-182 counteracts the aggravating effect of SIRT1 knockout on hepatic IR injury in mice by inhibiting the NLRP3 inflammatory pathway**

(A) Liver histomorphology of SIRT1 knockout mice treated with agomir NTC or miR-182 agomir, and scoring of the hepatic IR injury based on Suzuki et al.'s[19] standard (original magnification, ×400). (B) Serum ALT level of SIRT1 knockout mice treated with agomir NTC or miR-182 agomir as detected using a specific detection kit. (C) Expression of miR-182 in SIRT1 knockout mice treated with agomir NTC or miR-182 agomir as detected by qRT-PCR. (D) Protein expression of NLRP3 and C-caspase-1 in the liver of SIRT1 knockout mice treated with agomir NTC or miR-182 agomir as detected by western blot analysis. (E) The levels of IL-1β, TNF-α, and IL-18 in the serum of SIRT1 knockout mice treated with agomir NTC or miR-182 agomir as detected by ELISA. *$p < 0.05$ versus SIRT1 knockout mice treated with agomir NTC, **$p < 0.01$ versus SIRT1 knockout mice treated with agomir NTC. The data are measurement data, presented as mean ± standard deviation. Data between two groups were compared using an unpaired t test. The experiment was independently repeated three times. n = 10.

University). After plasmid amplification and extraction, the cells were transfected according to the instructions for the Lipofectamine 3000 kit. The vector plasmid was used as the control, and the culture was continued for 24 h after transfection. After the efficiency of overexpression or interference was detected, the next experiment was carried out.

### Treatment of mouse hepatocytes with SIRT1 activator SRT1720 and RSV

Mouse hepatocytes were processed by 1 mmol/L SRT1720 (Selleck Chemicals, Houston, TX, USA) or 10 mmol/L RSV for 24 h. RNA and protein of the cells were extracted, and qRT-PCR and western blot analysis were used to detect the activation efficiency. DMSO was added to the medium as a control.

### TUNEL staining

Liver tissues were fixed with 4% paraformaldehyde, embedded in paraffin, and cut into 4-μm-thick sections. TUNEL staining was carried out using a one-step TUNEL apoptosis assay kit (C1086, Shanghai Beyotime Biotechnology, Shanghai, China). The sections were treated with 20 mg/L DNase-free protease K for 20 min, and then incubated for 1 h in a mixture of the fluorescent labeling solution and TdT enzyme at 37°C. The sections were rinsed with 1× PBS three times and then placed in blocking agent containing 4′,6-diamidino-2-phenylindole to stain the nuclei. The fluorescent fluorescence signals were captured under an inverted fluorescence microscope (TH4-200, Olympus, Tokyo, Japan). Six visual fields of each section were randomly selected for apoptosis measurement.

### H&E staining and histological analysis

Liver tissues were fixed with 4% paraformaldehyde, embedded in paraffin, and cut into 4-μm-thick sections. The histomorphology analysis was carried out using H&E staining. The section images were observed and image by a Leica Microsystems DM2000 microscope (CMS, Wetzlar, Germany). Six visual fields of each section were randomly selected to evaluate liver injury. According to the standard proposed by Suzuki et al.,[19] three representative indexes of liver injury (congestion, vacuolation, and necrosis) were rated from 0 to 4 based on the severity (0 for none; 1 for extremely mild; 2 for mild; 3 for moderate; 4 for severe). Finally, the total score of the three representative measures for each section was counted and the score results were compared between each group.

### Immunohistochemistry

Liver tissues were fixed with 4% paraformaldehyde, embedded in paraffin, and cut into 4-μm-thick sections. The paraffin-embedded sections were treated with standard procedures for immunohistochemistry. The primary antibody (ab25989, Abcam, Cambridge, UK) to MPO and the horseradish peroxidase-labeled secondary antibody were successively used for section incubation. Then, 3,3′-diaminobenzidine staining was performed to observe the binding degree of the antibodies. Tissue sections were counterstained with hematoxylin, after which the section images were captured using the Leica Microsystems DM2000 microscope (CMS, Wetzlar, Germany). Six visual fields of each section were randomly selected through ImagePro Plus 6.0 (Media Cybernetics, Rockville, MD, USA). The cumulative IOD and area were calculated and the average IOD value was analyzed.

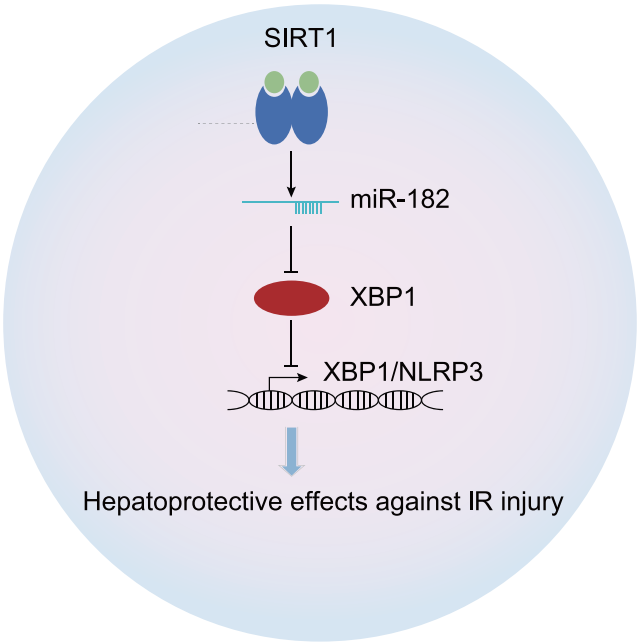


**Figure 10. Schematic map concerning the hepatoprotective mechanisms of the SIRT1 in hepatic IR injury**

SIRT1 might be an important mediator of these beneficial effects. SIRT1 ablation promotes hepatic IR injury by impairing miR-182-mediated XBP1/NLRP3 pathway inactivation.

### qRT-PCR

Total RNA was extracted from liver tissues stored in a refrigerator at −80°C using TRIzol reagent (Thermo Fisher Scientific, Waltham, MA, USA) according to the standard instructions followed by quantification through NanoDrop. The total RNA (1 μg) was reversely transcribed into complementary DNA (cDNA) by oligo(dT) primers and RTs using the RT kit of a HiScript III first-strand cDNA synthesis kit (MR101-01, R312-01, Vazyme). The relative mRNA expression was analyzed by comparing the threshold cycle with glyceraldehyde-3-phosphate dehydrogenase (GAPDH) and U6 as the internal references. The qPCR was conducted using the ChamQ SYBR color qPCR master mix (high ROX premixed) kit (Q441-02, Vazyme) in the StepOnePlus (Applied Biosystems, CA, USA). The primers used are presented in Table 1.

### Western blot analysis

The total protein extract was prepared with the liver tissue homogenates using radioimmunoprecipitation assay (RIPA) lysis buffer (the ratio of liver tissues and RIPA lysis buffer was 50 mg/1 mL). The protein concentration of the extracted homogenates was determined with the use of a bicinchoninic acid protein concentration detection kit. Extracts were resolved by sodium dodecyl sulfate-polyacrylamide gel electrophoresis, electroblotted onto polyvinylidene fluoride membranes (0.45 μm), and probed at 4°C overnight along with primary antibodies, followed by incubation with horseradish peroxidase-conjugated goat anti-rabbit or anti-mouse secondary antibodies. GAPDH was regarded as the internal reference for total protein expression and histone H3 for nuclear protein expression. Blots were developed using enhanced chemiluminescence reagent, and band areas were quantified using ImageJ software (US National Institutes of Health, Bethesda, MD, USA). The antibodies used in the experiment were as follows: SIRT1 (8469S, Cell Signaling Technology, Beverly, MA, USA), GAPDH (5174S, Cell Signaling Technology, Beverly, MA, USA), XBP1 (27901S, Cell Signaling Technology, Beverly, MA, USA), NLRP3 (15101S, Cell Signaling Technology, Beverly, MA, USA), ASC (13833S, Cell Signaling Technology, Beverly, MA, USA), C-caspase-1 (3866S, Cell Signaling Technology, Beverly, MA, USA), NF-κB (8242S, Cell Signaling Technology, Beverly, MA, USA).

### Chromatin immunoprecipitation (ChIP) assay

ChIP was conducted according to the instructions of a ChIP assay kit (Beyotime, P2078), as previously described.[37]

### ELISA

The bronchoalveolar lavage (BAL) BSA (1:5,000) was diluted with carbonate buffer solution (CBS, 0.05 mol/L, pH 9.6) and coated onto 96-well plates (100 μL/well). After 2 h of incubation at 37°C, the plate was washed four times with PBS and blocked (250 μL/well) with skimmed milk powder (5 g in 100 mL of deionized water). After being blocked in a refrigerator at 4°C overnight, the plate was washed three times with PBS followed by addition of the sample solution at a density of 50 μL/well and incubation at 37°C for 1 h. The wells with a control mass concentration of 0 were used as positive control wells. Enzyme-labeled secondary antibodies diluted in PBS (1:10,000) were added, 100 μL/well, and incubated at 37°C for 30 min. After incubation, the plate was washed three times with PBS and added with 100 μL of tetramethylbenzidine (TMB) solution for visualization at 37°C for 15 min. The reaction was stopped with 2 mol/L sulfuric acid solution (50 μL/well). The absorbance at 450 nm of each well was detected by a microplate reader to plot a curve. Finally, the protein concentration was calculated according to the curve and formula.

### Microarray analysis of the miRNA expression profile in liver tissues

Initially, 0.2 g of liver tissues was extracted and added with 1 mL of RNA extraction reagent TRIzol. After lysis, the RNA was extracted, and its concentration and quality were measured with NanoDrop. The purity of the RNA was evaluated, and the concentration was calculated by measuring the optical density of RNA at 230, 280, and 260 nm of the spectrophotometer. The miRNA molecules in the experimental sample RNA (the RNA samples used for chip detection were of high quality and complete, without RNase and genome pollution) were subjected to fluorescent labeling and hybridization. These procedures were further used in the hybridization experiment of the samples. After hybridization, the sections were washed in a washing tank with gene expression wash buffer reagent. The microarray results were scanned using an Agilent microarray scanner (catalog #G2565BA, Agilent Technologies, Santa Clara, CA, USA). The data were read using the feature extraction software 10.7

**Table 1. Primer sequences**

| | Primer sequences (5′→3′) |
|---|---|
| GAPDH | F: CGCTAACATCAAATGGGGTG |
| | R: TTGCTGACAATCTTGAGGGAG |
| SIRT1 | F: TAGCCTTGTCAGATAAGGAAGGA |
| | R: ACAGCTTCACAGTCAACTTTGT |
| XBP1 | F: CCCTCCAGAACATCTCCCCAT |
| | R: ACATGACTGGGTCCAAGTTGT |
| NLRP3 | F: GATCTTCGCTGCGATCAACAG |
| | R: CGTGCATTATCTGAACCCCAC |
| miR-182 | F: GCCGAGUGGUUCUAGACUUGCC |
| | R: CTCAACTGGTGTCGTGGA |
| mmu-miR-182-p | F: GAATTGGTACCCCTTGGTGGAGGCT TTGCTGAGACC |
| | R: GGAATACGCGTCAGCAGCCAGACCA GTAAGCCTATG |
| U6 | ATGGACTATCATATGCTTACCGTA |

(Agilent Technologies). Finally, GeneSpring software 11.0 (Agilent Technologies) was applied for quantile normalization.

### Dual-luciferase reporter gene assay

Using mouse genomic DNA as a template, 2,000-bp DNA fragments containing mouse miR-182 in the putative promoter region were amplified by PCR. The fragments were cloned into pGL3 luciferase reporter vector. Next, miR-182-Luc reporter plasmids (200 ng) containing luciferase gene and pRL-TK (50 ng) (Promega, Madison, WI, USA) were co-transfected with SIRT1 or control vectors (800 ng) into human HEK293T cells. The luciferase activity was measured using a dual-luciferase reporter system (Promega, Madison, WI, USA) and a Centro LB 960 detection system.

The UTR of mouse XBP1 containing the putative target site of miR-182 was amplified from mouse genomic DNA through PCR and inserted into pmiR-REPORT (Ribobio, Guangzhou, China) The mutant type (MUT) reporter plasmid of the miR-182 complementary site (TGCCAAA to ACGGTTT) was produced by a QuikChange II site-directed mutagenesis kit. SHSY5Y neuroblastoma cells were transiently transfected with WT or MUT reporter plasmids and miRNA agomir with the use of Lipofectamine 2000 (Invitrogen, Carlsbad, CA, USA). The primers used are shown in Table 1.

### Statistical analysis

Data analysis was performed with the use of SPSS 21.0 (IBM, Armonk, NY, USA). Measurement data were presented as mean ± standard deviation. An unpaired t test was applied to compare the unpaired data between two groups, obeying normal distribution and homogeneity of variance. Data among multiple groups were compared using one-way analysis of variance (ANOVA), with a Tukey's test conducted for a post hoc test. A p value of $<0.05$ was indicative of a statistically significant difference.

## ACKNOWLEDGMENTS

We acknowledge and appreciate our colleagues for their technical assistance. This work was supported by the State Key Project on Infectious Diseases of China (grant no. 2018ZX10723204); the Joint Tackling Project of Emerging Frontier Technologies in Shanghai Hospitals in 2017 (grant no. SHDC12017122); the National Natural Science Foundation of China (grant no. 81970636); and by the Key Breakthrough Direction of Special Disease of Navy Medical University Investigative-Oriented Department and Investigative Type Doctor Construction Project in 2017 (to K.W. and Yong Xia).

## AUTHOR CONTRIBUTIONS

F.L. and L.Z. performed experiments and interpreted results of experiments. H.X. analyzed data. J.X. prepared figures. K.W. designed the research and drafted paper. S.R. edited and revised the manuscript. All authors read and approved the final version of the manuscript.

## DECLARATIONS OF INTEREST

The authors declare no competing interests.

## REFERENCES

1. Guo, W.Z., Fang, H.B., Cao, S.L., Chen, S.Y., Li, J., Shi, J.H., Tang, H.W., Zhang, Y., Wen, P.H., Zhang, J.K., et al. (2020). Six-transmembrane epithelial antigen of the prostate 3 deficiency in hepatocytes protects the liver against ischemia-reperfusion injury by suppressing transforming growth factor-β-activated kinase 1. Hepatology *71*, 1037–1054.
2. Wu, W., Wu, Y., Cheng, G., Zhang, C., Wang, H., and Li, Y. (2019). A mouse model of hepatic ischemia-reperfusion injury demonstrates potentially reversible effects on hippocampal neurons and postoperative cognitive function. Med. Sci. Monit. *25*, 1526–1536.
3. Yan, Z.Z., Huang, Y.P., Wang, X., Wang, H.P., Ren, F., Tian, R.F., Cheng, X., Cai, J., Zhang, Y., Zhu, X.Y., et al. (2019). Integrated omics reveals Tollip as an regulator and therapeutic target for hepatic ischemia-reperfusion injury in mice. Hepatology *70*, 1750–1769.
4. Pan, W., Wang, L., Zhang, X.F., Zhang, H., Zhang, J., Wang, G., Xu, P., Zhang, Y., Hu, P., Zhang, X.D., et al. (2019). Hypoxia-induced microRNA-191 contributes to hepatic ischemia/reperfusion injury through the ZONAB/cyclin D1 axis. Cell Death Differ. *26*, 291–305.
5. Weiss, T.S., Lupke, M., Dayoub, R., Geissler, E.K., Schlitt, H.J., Melter, M., and Eggenhofer, E. (2019). Augmenter of liver regeneration reduces ischemia reperfusion injury by less chemokine expression, Gr-1 infiltration and oxidative stress. Cells *8*, 1421.
6. Inoue, Y., Yasuda, Y., and Takahashi, M. (2013). Role of the inflammasome in inflammatory responses and subsequent injury after hepatic ischemia-reperfusion injury. Hepatology *58*, 2212.
7. Kobayashi, M. (1989). [Epidemiological study on tuberculosis in Tochigi Prefecture. Part I: Factor relating to the onset of tuberculosis in three health centers of Tochigi Prefecture]. Kekkaku *64*, 605–612.
8. Zhang, N., Han, L., Xue, Y., Deng, Q., Wu, Z., Peng, H., Zhang, Y., Xuan, L., Pan, G., and Fu, Q. (2019). The protective effect of magnesium lithospermate B on hepatic ischemia/reperfusion *via* inhibiting the Jak2/Stat3 signaling pathway. Front. Pharmacol. *10*, 620.
9. Jiang, X., Kuang, G., Gong, X., Jiang, R., Xie, T., Tie, H., Wu, S., Wang, T., Wan, J., and Wang, B. (2019). Glycyrrhetinic acid pretreatment attenuates liver ischemia/reperfusion injury via inhibiting TLR4 signaling cascade in mice. Int. Immunopharmacol. *76*, 105870.
10. Zheng, D., Li, Z., Wei, X., Liu, R., Shen, A., He, D., Tang, C., and Wu, Z. (2018). Role of miR-148a in mitigating hepatic ischemia-reperfusion injury by repressing the TLR4 signaling pathway via targeting CaMKIIα in vivo and in vitro. Cell. Physiol. Biochem. *49*, 2060–2072.

11. Xiong, L., Yu, K.H., and Zhen, S.Q. (2018). miR-93 blocks STAT3 to alleviate hepatic injury after ischemia-reperfusion. Eur. Rev. Med. Pharmacol. Sci. *22*, 5295–5304.

12. Jiang, W., Liu, G., and Tang, W. (2016). MicroRNA-182-5p ameliorates liver ischemia-reperfusion injury by suppressing Toll-like receptor 4. Transplant. Proc. *48*, 2809–2814.

13. Wang, J., Xu, Z., Chen, X., Li, Y., Chen, C., Wang, C., Zhu, J., Wang, Z., Chen, W., Xiao, Z., and Xu, R. (2018). MicroRNA-182-5p attenuates cerebral ischemia-reperfusion injury by targeting Toll-like receptor 4. Biochem. Biophys. Res. Commun. *505*, 677–684.

14. Wang, Y., Zhao, X., Wu, X., Dai, Y., Chen, P., and Xie, L. (2016). MicroRNA-182 mediates Sirt1-induced diabetic corneal nerve regeneration. Diabetes *65*, 2020–2031.

15. Nakamura, K., Kageyama, S., Ke, B., Fujii, T., Sosa, R.A., Reed, E.F., Datta, N., Zarrinpar, A., Busuttil, R.W., and Kupiec-Weglinski, J.W. (2017). Sirtuin 1 attenuates inflammation and hepatocellular damage in liver transplant ischemia/reperfusion: from mouse to human. Liver Transpl. *23*, 1282–1293.

16. Li, Y., Yang, X., He, Y., Wang, W., Zhang, J., Zhang, W., Jing, T., Wang, B., and Lin, R. (2017). Negative regulation of NLRP3 inflammasome by SIRT1 in vascular endothelial cells. Immunobiology *222*, 552–561.

17. Inoue, Y., Shirasuna, K., Kimura, H., Usui, F., Kawashima, A., Karasawa, T., Tago, K., Dezaki, K., Nishimura, S., Sagara, J., et al. (2014). NLRP3 regulates neutrophil functions and contributes to hepatic ischemia-reperfusion injury independently of inflammasomes. J. Immunol. *192*, 4342–4351.

18. Olivares, S., and Henkel, A.S. (2015). Hepatic *Xbp1* gene deletion promotes endoplasmic reticulum stress-induced liver injury and apoptosis. J. Biol. Chem. *290*, 30142–30151.

19. Suzuki, S., Toledo-Pereyra, L.H., Rodriguez, F.J., and Cejalvo, D. (1993). Neutrophil infiltration as an important factor in liver ischemia and reperfusion injury. Modulating effects of FK506 and cyclosporine. Transplantation *55*, 1265–1272.

20. Anger, F., Camara, M., Ellinger, E., Germer, C.T., Schlegel, N., Otto, C., and Klein, I. (2019). Human mesenchymal stromal cell-derived extracellular vesicles improve liver regeneration after ischemia reperfusion injury in mice. Stem Cells Dev. *28*, 1451–1462.

21. Mohammed, S.G., Ibrahim, I.A.A.E., Mahmoud, M.F., and Mahmoud, A.A.A. (2019). Carvedilol protects against hepatic ischemia/reperfusion injury in high-fructose/high-fat diet-fed mice: role of G protein-coupled receptor kinase 2 and 5. Toxicol. Appl. Pharmacol. *382*, 114750.

22. Pantazi, E., Folch-Puy, E., Bejaoui, M., Panisello, A., Varela, A.T., Rolo, A.P., Palmeira, C.M., and Roselló-Catafau, J. (2015). PPARα agonist WY-14643 induces SIRT1 activity in rat fatty liver ischemia-reperfusion injury. BioMed Res. Int. *2015*, 894679.

23. Shalwala, M., Zhu, S.G., Das, A., Salloum, F.N., Xi, L., and Kukreja, R.C. (2014). Sirtuin 1 (SIRT1) activation mediates sildenafil induced delayed cardioprotection against ischemia-reperfusion injury in mice. PLoS ONE *9*, e86977.

24. Nakamura, K., Zhang, M., Kageyama, S., Ke, B., Fujii, T., Sosa, R.A., Reed, E.F., Datta, N., Zarrinpar, A., Busuttil, R.W., et al. (2017). Macrophage heme oxygenase-1-SIRT1-p53 axis regulates sterile inflammation in liver ischemia-reperfusion injury. J. Hepatol. *67*, 1232–1242.

25. Shigeoka, A.A., Mueller, J.L., Kambo, A., Mathison, J.C., King, A.J., Hall, W.F., Correia, Jda.S., Ulevitch, R.J., Hoffman, H.M., and McKay, D.B. (2010). An inflammasome-independent role for epithelial-expressed Nlrp3 in renal ischemia-reperfusion injury. J. Immunol. *185*, 6277–6285.

26. He, Q., Li, Z., Wang, Y., Hou, Y., Li, L., and Zhao, J. (2017). Resveratrol alleviates cerebral ischemia/reperfusion injury in rats by inhibiting NLRP3 inflammasome activation through Sirt1-dependent autophagy induction. Int. Immunopharmacol. *50*, 208–215.

27. Ma, C.H., Kang, L.L., Ren, H.M., Zhang, D.M., and Kong, L.D. (2015). Simiao pill ameliorates renal glomerular injury via increasing Sirt1 expression and suppressing NF-κB/NLRP3 inflammasome activation in high fructose-fed rats. J. Ethnopharmacol. *172*, 108–117.

28. Li, C., Jin, Y., Wei, S., Sun, Y., Jiang, L., Zhu, Q., Farmer, D.G., Busuttil, R.W., Kupiec-Weglinski, J.W., and Ke, B. (2019). Hippo signaling controls NLR family pyrin domain containing 3 activation and governs immunoregulation of mesenchymal stem cells in mouse liver injury. Hepatology *70*, 1714–1731.

29. Liu, L., Xu, L., Zhang, S., Wang, D., Dong, G., Chen, H., Li, X., Shu, C., and Wang, R. (2018). STF-083010, an inhibitor of XBP1 splicing, attenuates acute renal failure in rats by suppressing endoplasmic reticulum stress-induced apoptosis and inflammation. Exp. Anim. *67*, 373–382.

30. Lee, S.Y., Lee, S., Choi, E., Ham, O., Lee, C.Y., Lee, J., Seo, H.H., Cha, M.J., Mun, B., Lee, Y., et al. (2016). Small molecule-mediated up-regulation of microRNA targeting a key cell death modulator BNIP3 improves cardiac function following ischemic injury. Sci. Rep. *6*, 23472.

31. Ding, X.Q., Wu, W.Y., Jiao, R.Q., Gu, T.T., Xu, Q., Pan, Y., and Kong, L.D. (2018). Curcumin and allopurinol ameliorate fructose-induced hepatic inflammation in rats via miR-200a-mediated TXNIP/NLRP3 inflammasome inhibition. Pharmacol. Res. *137*, 64–75.

32. Jimenez Calvente, C., Del Pilar, H., Tameda, M., Johnson, C.D., and Feldstein, A.E. (2020). MicroRNA 223 3p negatively regulates the NLRP3 inflammasome in acute and chronic liver injury. Mol. Ther. *28*, 653–663.

33. Purushotham, A., Schug, T.T., Xu, Q., Surapureddi, S., Guo, X., and Li, X. (2009). Hepatocyte-specific deletion of SIRT1 alters fatty acid metabolism and results in hepatic steatosis and inflammation. Cell Metab. *9*, 327–338.

34. Li, M., Hong, W., Hao, C., Li, L., Wu, D., Shen, A., Lu, J., Zheng, Y., Li, P., and Xu, Y. (2018). SIRT1 antagonizes liver fibrosis by blocking hepatic stellate cell activation in mice. FASEB J. *32*, 500–511.

35. Purushotham, A., Xu, Q., Lu, J., Foley, J.F., Yan, X., Kim, D.H., Kemper, J.K., and Li, X. (2012). Hepatic deletion of SIRT1 decreases hepatocyte nuclear factor 1α/farnesoid X receptor signaling and induces formation of cholesterol gallstones in mice. Mol. Cell. Biol. *32*, 1226–1236.

36. Jiménez-Castro, M.B., Cornide-Petronio, M.E., Gracia-Sancho, J., and Peralta, C. (2019). Inflammasome-mediated inflammation in liver ischemia-reperfusion injury. Cells *8*, 1131.

37. He, Y., Lu, J., Ye, Z., Hao, S., Wang, L., Kohli, M., Tindall, D.J., Li, B., Zhu, R., Wang, L., and Huang, H. (2018). Androgen receptor splice variants bind to constitutively open chromatin and promote abiraterone-resistant growth of prostate cancer. Nucleic Acids Res. *46*, 1895–1911.